N2–N2 interaction potential from a b i n i t i o calculations, with application to the structure of (N2)2

Rut M. Berns and Ad van der Avoird

Citation: The Journal of Chemical Physics **72**, 6107 (1980); doi: 10.1063/1.439067
View online: http://dx.doi.org/10.1063/1.439067
View Table of Contents: http://scitation.aip.org/content/aip/journal/jcp/72/11?ver=pdfcov
Published by the AIP Publishing

N_2–N_2 interaction potential from *ab initio* calculations, with application to the structure of $(N_2)_2$ [a)]

Rut M. Berns and Ad van der Avoird

Institute of Theoretical Chemistry, University of Nijmegen, Toernooiveld, Nijmegen, The Netherlands
(Received 22 January 1980; accepted 19 February 1980)

The short range electrostatic and (first order) exchange contributions to the N_2–N_2 interaction energy have been calculated *ab initio* as a function of the N_2 orientations and the distance (139 geometries). Using a numerical integration procedure, the results have been represented analytically in the form of a spherical expansion. At $R = 0.3$ nm this expansion is accurate to better than 0.5% if we include the first 18 independent terms, to 2% if we truncate after $L_A = L_B = 4$, and to 16% if we truncate after $L_A = L_B = 2$. In combination with the long range multipole expansion results (electrostatic R^{-5}, R^{-7}, R^{-9} terms, dispersion R^{-6}, R^{-8}, R^{-10} terms) calculated by Mulder *et al.*, this yields an anisotropic N_2–N_2 interaction potential in the region of the van der Waals minimum, which can be fairly well represented also by a site–site model. The potential is in good agreement with the available experimental data for the gas phase and for the ordered (α and γ) crystal phases of solid N_2. The structure of the van der Waals molecule $(N_2)_2$ is discussed; its energy is lowest for the crossed structure: $\Delta E_m = 1.5$ kJ/mol, $R_m = 0.35$ nm (for the isotropic potential the well characteristics are $\Delta E_m = 0.75$ kJ/mol and $R_m = 0.417$ nm). The (staggered) parallel and the T-shaped structures are slightly higher in energy. The internal N_2 rotation barriers vary from 0.2 kJ/mol (17 cm^{-1}) to values comparable with the dissociation energy.

I. INTRODUCTION

Knowledge of the intermolecular interaction potential is basic for understanding the properties of molecular gases, liquids, and solids. In principle, this interaction potential can be derived from experimental sources. In practice one has to introduce model potentials with a limited number of parameters and then fit these parameters to the experimental data. For nitrogen, much work has been done in this direction (see Refs. 1 and 2) using gas phase data (virial coefficients, viscosity data) as well as solid state properties (from x-ray diffraction, IR, Raman, and nuclear resonance spectroscopy, neutron scattering). Model potentials which have been used[1,2] are molecular ones, isotropic or elliptical, and atom–atom potentials, with distance dependent functions mostly of the Lennard–Jones (12-6) or Buckingham (exp -6) type. Sometimes, these have been supplemented with the electrostatic quadrupole–quadrupole interaction.[2] In spite of all these efforts, there is still no N_2–N_2 interaction potential available at present that is universal in the sense that it fits all the different experimental data. Especially, the anisotropy of the potential, its dependence on the relative N_2–N_2 orientations, has not been established unequivocally.

Another way to determine the N_2–N_2 interaction potential is by *ab initio* calculations. Such calculations, which yield the anisotropic interactions, have been performed by Mulder *et al.*[3] in the long range region where the interaction potential can be expanded as a multipole series, i. e., in powers of the distance R. Here, we report results for shorter distances, including the physically important region around the van der Waals minimum. These have been obtained from *ab initio* calculations which avoid the multipole expansion of the interaction operator and which take the intermolecular exchange into account (in first order). The results are given for a set of intermolecular distances and molecular orientations, but, we also present two analytical representations of the interaction potential. The first one is a spherical expansion in terms of the angles describing the molecular orientations. Such an expansion is obtained directly in the long range if one substitutes a spherical multipole expansion into the Rayleigh–Schrödinger perturbation expressions for the interaction energy[4,5]; in the short range a fitting or numerical integration procedure is required, which we describe. Also, we discuss the convergence of this spherical expansion. The second approximate representation of the *ab initio* results is in the form of an atom–atom potential.

II. *AB INITIO* CALCULATIONS AND RESULTS

The interaction energy between two N_2 molecules A and B has been calculated in a general space fixed coordinate system as a function of the orientations, described by the polar coordinates $\omega_A = (\theta_A, \phi_A)$ and $\omega_B = (\theta_B, \phi_B)$, and the distance vector $\mathbf{R} = (R, \Omega) = (R, \Theta, \Phi)$. In order to simplify the calculations, we have chosen a special frame with the z axis along $\mathbf{R}$ ($\Theta = \Phi = 0$) and molecule B in the xz plane ($\phi_B = 0$), and we have varied only the "internal" coordinates, R, θ_A, θ_B, ϕ_A. The energy has been calculated up to second order in perturbation theory.

(a) The first order interaction energy, including exchange, is defined as:

$$\Delta E^{(1)}(\omega_A, \omega_B, \mathbf{R}) = \langle \mathcal{A}\psi_0^A\psi_0^B \,|\, H^{AB} \,|\, \mathcal{A}\psi_0^A\psi_0^B \rangle - \langle \psi_0^A \,|\, H^A \,|\, \psi_0^A \rangle - \langle \psi_0^B \,|\, H^B \,|\, \psi_0^B \rangle . \quad (1)$$

The nitrogen monomer wave functions ψ_0^A and ψ_0^B have been taken as ground state Hartree–Fock molecular orbital–linear combination of atomic orbital (MO-LCAO) functions (Slater determinants). The N–N distance was fixed at the experimental value of 0.1094 nm.[6] The operators H^{AB}, H^A, and H^B are the dimer and

[a)]Supported in part by the Netherlands Foundation for Chemical Research (SON) with financial aid from the Netherlands Organization for the Advancement of Pure Research (ZWO).

 0021-9606/80/116107-10$01.00

monomer Hamiltonians, respectively; $\mathcal{A}$ is the normalized antisymmetrizer of the dimer. For the expansion of the MO's the atomic orbital (AO) basis set D of Mulder *et al.*,[3] including two d-type polarization functions, has been used. This large basis is necessary in order to obtain reliable molecular multipole moments.[3]

This first order energy $\Delta E^{(1)}$ can be separated into an electrostatic component, $\Delta E^{(1)}_{\text{elec}}$, defined by (1) with the operator $\mathcal{A}$ replaced by the identity, and an exchange component defined as

$$\Delta E^{(1)}_{\text{exch}} = \Delta E^{(1)} - \Delta E^{(1)}_{\text{elec}} .$$

For large intermolecular distances, one can approximate $\Delta E^{(1)}_{\text{elec}}$ by a power series in R by substituting the multipole expansion for the interaction operator $V^{AB} = H^{AB} - H^A - H^B$:

$$\Delta E^{(1)}_{\text{mult}} = \sum_n C_n(\omega_A, \omega_B, \Omega) R^{-n}$$

with $n = 5$, 7, 9, etc. Actually, this expansion is an asymptotic series. The deviation $\Delta E^{(1)}_{\text{pen}} = \Delta E^{(1)}_{\text{elec}} - \Delta E^{(1)}_{\text{mult}}$ is due to the penetration between the charge clouds of the two nitrogen molecules, which increases exponentially with decreasing distance.

(b) The second order interaction energy, without exchange, is defined as:

$$\Delta E^{(2)} = \sum_{a,b\neq 0,0} \frac{|\langle \psi_0^A \psi_0^B | V^{AB} | \psi_a^A \psi_b^B \rangle|^2}{E_0^A - E_a^A + E_0^B - E_b^B} . \qquad (2)$$

The second order exchange energy has been neglected as it is rather small in the region around the van der Waals minimum for those cases where it has been evaluated.[7] The excited monomer wave functions, ψ_a^A and ψ_b^B, are constructed by exciting one electron to a virtual ground state Hartree–Fock MO; the energy differences in the denominator are replaced by orbital energy differences. This choice is sometimes called the uncoupled Hartree–Fock perturbation method.[8] The same method and some other perturbation methods have been applied to the long range N_2–N_2 interaction energy by Mulder *et al.*,[3] who also discussed the quantitative defects of these methods. The second order energy can be separated into an induction and a dispersion part:

$$\Delta E^{(2)} = \sum_{a,b\neq 0,0} \cdots = \sum_{\substack{a\neq 0 \\ b=0}} \cdots + \sum_{\substack{a=0 \\ b\neq 0}} \cdots + \sum_{\substack{a\neq 0 \\ b\neq 0}} \cdots$$

$$= \Delta E^{(2)}_{\text{ind}\,A} + \Delta E^{(2)}_{\text{ind}\,B} + \Delta E^{(2)}_{\text{disp}} = \Delta E^{(2)}_{\text{ind}} + \Delta E^{(2)}_{\text{disp}} .$$

For large intermolecular distances one can again substitute the multipole expansion for V^{AB} and obtain the series:

$$\Delta E^{(2)}_{\text{mult}} = \sum_n C_n(\omega_A, \omega_B, \Omega) R^{-n}$$

with $n = 6$, 8, 10, etc. The charge penetration effect is defined by the difference

$$\Delta E^{(2)}_{\text{pen}} = \Delta E^{(2)} - \Delta E^{(2)}_{\text{mult}} .$$

For the calculation of the second order energy the MO's have been expanded in the basis G' of Mulder *et al.*[3] which contains d and f type atomic polarization functions. The addition of f functions to the first order basis D, but, also, a somewhat different optimization of the orbital exponents, is necessary in order to ensure approximate completeness of the excited state wave functions, ψ_a^A and ψ_b^B.[3,9]

TABLE I. First order interaction energy contributions.

Geometry[a] θ_A, θ_B, ϕ_A R(nm)	$\Delta E^{(1)}$[b] (kJ mol^{-1})	$\Delta E^{(1)}_{\text{exch}}$[b] (kJ mol^{-1})	$\Delta E^{(1)}_{\text{elec}}$[b] (kJ mol^{-1})	$\Delta E^{(1)}_{\text{mult}}$[c] (kJ mol^{-1})
90°, 90°, 0°				
0.331	3.991	4.481	−0.490	0.375
0.357	1.562	1.564	−0.002	0.259
0.384	0.640	0.531	0.109	0.187
0.410	0.291	0.176	0.115	0.139
0.437	0.154	0.056	0.098	0.105
90°, 90°, 90°				
0.331	3.519	4.154	−0.635	0.134
0.357	1.331	1.461	−0.130	0.096
0.384	0.505	0.499	0.006	0.071
0.410	0.201	0.166	0.035	0.053
0.437	0.089	0.054	0.035	0.040
45°, 45°, 0°				
0.331	15.619	21.689	−6.070	−0.649
0.357	5.753	7.985	−2.232	−0.467
0.384	1.975	2.855	−0.880	−0.337
0.410	0.588	0.992	−0.404	−0.246
0.437	0.109	0.335	−0.226	−0.182
45°, 135°, 0°				
0.331	27.187	35.132	−7.945	1.391
0.357	10.440	12.508	−2.068	0.889
0.384	4.045	4.340	−0.295	0.593
0.410	1.625	1.469	0.156	0.409
0.437	0.706	0.484	0.222	0.291
0°, 0°, 0°				
0.331	104.589	142.630	−38.041	4.177
0.357	43.925	55.629	−11.704	2.525
0.384	15.959	18.882	−2.923	1.601
0.410	6.299	6.600	−0.301	1.057
0.437	2.586	2.249	0.337	0.721
0.463	1.152			
0.489	0.582			
0.516	0.340			
0.542	0.224			
0°, 90°, 0°				
0.331	17.515	24.113	−6.598	−0.747
0.357	6.345	8.718	−2.373	−0.533
0.384	2.133	3.067	−0.934	−0.384
0.410	0.613	1.050	−0.437	−0.280
0.437	0.099	0.349	−0.250	−0.208

[a] Coordinate system described in text; data for 105 additional orientations have been calculated at $R = 0.3$ nm (see Table IV).
[b] Monomer MO's and integrals calculated with the ATMOL3 program. We thank Dr. M. F. Guest, Daresbury Laboratory, UK, for making this program available to us and Mr. J. van Lierop for assistance with the implementation. Interaction energies evaluated with the program COULEX written by P. E. S. Wormer, Nijmegen. GTO basis set 9s, 5p, 2d contracted to 4s, 3p, 2d. (Basis D of Ref. 3.)
[c] Obtained from the multipole moments of Ref. 3, calculated in the same Basis D.

The first order interaction energy and its components have been calculated, in first instance, for six orientations and several distances of the N_2 molecules in the dimer (34 different geometries). The results are listed in Table I and plotted for two parallel N_2 molecules as a function of distance in Fig. 1. From these results we observe that the first order penetration and exchange effects are quite important already at the van der Waals

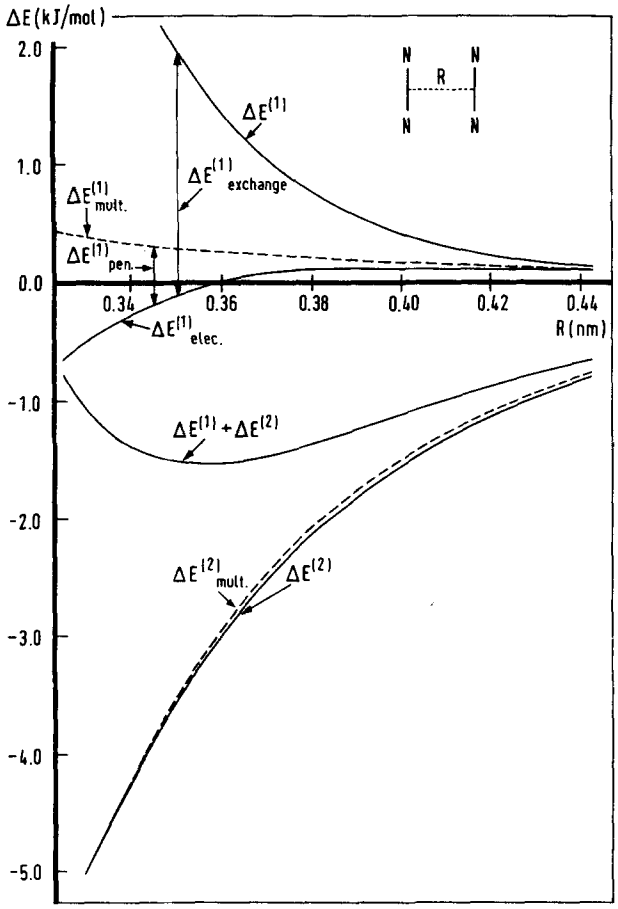

FIG. 1. Different contributions (as defined in the text) to the interaction energy between two parallel N_2 molecules; *ab initio* results, see Tables I and II.

minimum. (This minimum lies at $R=0.417$ nm for the isotropic potential, see below, and at $R=0.36$ nm for the parallel dimer, see Fig. 1). This conclusion agrees with the penetration effect calculations by Ng *et al.* [10]

The second order interaction energy has been calculated for ten geometries only, see Table II and Fig. 1. We have found, just as Mulder *et al.*, [3] that the induction energy can be neglected with respect to the dispersion energy. The second order penetration energy is much smaller than the corresponding first order contribution. Therefore, the second order energy can be well represented by the dispersion multipole series, $\Delta E^{(2)}_{\text{mult,disp}}$. Mulder *et al.* [3] have pointed out, however, that the dispersion multipole coefficients obtained by the uncoupled Hartree–Fock perturbation method (but also by other perturbation methods starting from Hartree–Fock monomer wave functions) are rather inaccurate for N_2–N_2. Using accurate semiempirical data for C_6 and for the dipole polarizability (from dipole oscillator strength distributions) in combination with their *ab initio* results, they have made better estimates for the higher multipole coefficients C_8 and C_{10} and the corresponding anisotropy factors. From here on, we shall use the latter results (Ref. 3, Table VI) in order to represent the second order N_2–N_2 interaction energy.

TABLE II. Second order interaction energy contributions.

Geometry[a] θ_A, θ_B, ϕ_A R(nm)	$\Delta E^{(2)}_{\text{ind}}$[b] (kJ mol^{-1})	$\Delta E^{(2)}_{\text{mult,ind}}$[c] (kJ mol^{-1})	$\Delta E^{(2)}_{\text{disp}}$[b] (kJ mol^{-1})	$\Delta E^{(2)}_{\text{mult,disp}}$[c] (kJ mol^{-1})
90°, 90°, 0°				
0.331	−0.070	−0.015	−5.045	−5.046
0.357	−0.018	−0.009	−3.074	−3.009
0.384	−0.007	−0.005	−1.931	−1.877
0.410	−0.003	−0.003	−1.250	−1.216
0.437	−0.002	−0.002	−0.833	−0.813
90°, 90°, 90°				
0.331	−0.066	−0.019	−4.606	−4.654
45°, 45°, 0°				
0.331	−1.462	−0.042	−10.162	−10.099
45°, 135°, 0°				
0.331	−2.858	−0.076	−12.528	−11.417
0°, 0°, 0°				
0.331	−17.996	−0.312	−24.899	−19.314
0°, 90°, 0°				
0.331	−1.250	−0.097	−10.033	−9.629

[a]Coordinate system defined in text.
[b]Monomer MO's and integrals calculated with the IBMOL package written by E. Clementi and co-workers; interaction energies with a program written by R. M. Berns, Nijmegen, which is a modification of the program written by T. P. Groen, Utrecht. GTO basis 9*s*, 5*p*, 2*d*, 1*f* contracted to 4*s*, 3*p*, 2*d*, 1*f* (basis *G'* of Ref. 3).
[c]Obtained from the multipole coefficients in Table IV of Ref. 3, which have been calculated with the same basis *G'*.

The total, first plus second order, interaction energies have been plotted in Fig. 2.

III. ANALYTICAL REPRESENTATION OF THE INTERACTION POTENTIAL

A. Spherical expansion

The dependence of the (anisotropic) interaction potential between two molecules A and B on the orientations of these molecules can be explicitly expressed in the form of a spherical expansion. [11–13] For two identical homonuclear diatomic molecules this expansion reads:

$$\Delta E(\omega_A, \omega_B, \mathbf{R}) = (4\pi)^{3/2} \sum_{\substack{L_A \geq L_B \\ (L_A, L_B, L \text{ even})}} \sum_{L} V_{L_A, L_B, L}(R)(2-\delta_{L_A, L_B}) \times \tfrac{1}{2}[A_{L_A, L_B, L}(\omega_A, \omega_B, \Omega) + A_{L_B, L_A, L}(\omega_A, \omega_B, \Omega)] \tag{3a}$$

with the angular functions given by:

$$A_{L_A, L_B, L}(\omega_A, \omega_B, \Omega) = \sum_{M_A, M_B, M} \begin{pmatrix} L_A & L_B & L \\ M_A & M_B & M \end{pmatrix} Y_{L_A, M_A}(\omega_A) Y_{L_B, M_B}(\omega_B) Y_{L, M}(\Omega) . \tag{3b}$$

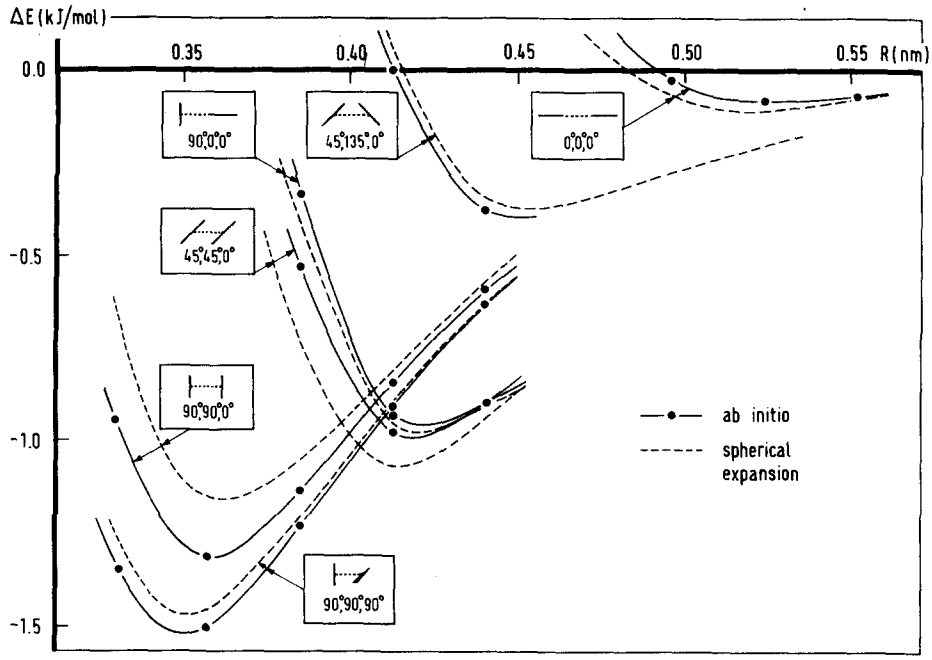

FIG. 2. Total interaction energy at six different orientations. *"Ab initio"*: first order energy from Table I, second order energy from the dispersion multipole coefficients of Ref. 3 (Table VI), see our Table V. Spherical expansion, see Table V.

The functions $Y_{L,M}(\omega)$ are spherical harmonics[14] which are coupled with the aid of a Wigner 3-j symbol

$$\begin{pmatrix} L_A & L_B & L \\ M_A & M_B & M \end{pmatrix}$$

to a scalar. That is, the angular functions $A_{L_A,L_B,L}$ are invariant under rotations of the total system.[13] The expansion coefficients, $V_{L_A,L_B,L}$, which are functions of the distance only, completely determine the orientational dependence of the intermolecular interaction potential. For a given potential $\Delta E(\omega_A, \omega_B, R)$ they can be expressed as:

$$V_{L_A,L_B,L}(R) = (4\pi)^{-3/2} \int d\omega_A \int d\omega_B \int d\Omega \times A_{L_A,L_B,L}(\omega_A, \omega_B, \Omega) \Delta E(\omega_A, \omega_B, R) . \quad (4)$$

Here, we have used the orthonormality of the angular functions $A_{L_A,L_B,L}$. Since $A_{0,0,0} \equiv (4\pi)^{-3/2}$ and $\int d\omega_A \times \int d\omega_B \int d\Omega = (4\pi)^3$, it is obvious that $V_{0,0,0}(R)$ is just the isotropic potential.

In the long range, where the multipole expansion for V^{AB} can be used, the first and second order interaction energies, $\Delta E^{(1)}_{mult}$ and $\Delta E^{(2)}_{mult}$, , are easily obtained in form (3). All one has to do is use an expansion of V^{AB} in terms of spherical multipoles[4]; in first order this leads directly to the result (3), in second order some angular momentum recoupling has to be done.[4,5] In both cases, the expansion coefficients $V_{L_A,L_B,L}(R)$ are simply powers of R^{-1} then, multiplied by constant coefficients $C_n^{L_A,L_B,L}$, which contain the properties of the systems A and B (multipole moments in first order, multipole transition moments and excitation energies in second order). These multipole coefficients have been calculated for N_2–N_2 by Mulder *et al.*[3] So, the present paper only deals with the spherical expansion of the (*ab initio*) calculated short range interactions, $\Delta E^{(1)}_{pen}$ and $\Delta E^{(1)}_{exch}$.

At first we have tried a procedure which has been used for H_2–He (Refs. 15 and 16) and H_2–H_2.[17] From the interaction energy calculated for five different orientations (at a given distance R) we have computed the first five spherical expansion coefficients: $V_{0,0,0}$, $V_{2,0,2}$, $V_{2,2,0}$, $V_{2,2,2}$, $V_{2,2,4}$. This simply involves the solution of a system of five simultaneous linear equations. The results for the sixth orientation have been used as a check on the accuracy of the expansion coefficients. This procedure has been repeated for different choices of orientations, but the results were always poor. So we concluded that, either the spherical expansion is far from having converged with these first five terms, or the applied procedure is not numerically stable (if the remaining terms in the expansion are small but not negligible), or both. In order to investigate these questions we have proceeded as follows.

B. Atom–atom representation of the *ab initio* potential

The interaction energy between the two N_2 molecules has been approximated by an atom–atom potential:

$$\Delta E^{AB} = \sum_{i \in A} \sum_{j \in B} V_{ij}$$

with V_{ij} being dependent only on the distance r_{ij} between the atoms:

$$V_{ij}(r_{ij}) = q_i q_j r_{ij}^{-1} - C_{ij} r_{ij}^{-6} + A_{ij} \exp(-B_{ij} r_{ij}) .$$

The electrostatic interaction potential, which is added to the Buckingham (exp-6) potential, depends on the charges q_i, q_j of the atoms. It is obvious that this model as such cannot represent the electrostatic interaction between N_2 molecules, since the atomic charges should be zero. Therefore, we have chosen for a generalized atom–atom (site–site) model with two positive and two negative charges (of equal magnitude) placed symmetrically on the N–N axis. Also the force centers

TABLE III. Atom–atom potential fitted to the "*ab initio*" data.

	Parameters	I fit for $0.33 \leq R \leq 0.44$ nm	II fit for $0.30 \leq R \leq 0.44$ nm
Electrostatic:	charges[a] $q = q_+ = -q_-$	$0.373e$[b]	$0.379e$[b]
	positions[a] z_+, z_- (nm)	± 0.0847, ± 0.1044	± 0.0848, ± 0.1041
Short range repulsion: (exchange + penetration)	A (kJ mol^{-1})	770 000	559 000
	B (nm^{-1})	40.37	39.49
	force centers[c] z_{SR}(nm)	± 0.0547	± 0.0547
Dispersion:	C (kJ mol^{-1} nm^6)	0.001511(0.001407)[d]	
	force centers z_D (nm)	± 0.0471	

[a]Molecular multipole moments calculated with this point charge model: $Q_{2,0} = -4.449\ 10^{-40}\ C\ m^2$, $Q_{4,0} = -8.046\ 10^{-60}\ C\ m^4$, $Q_{6,0} = -11.063\ 10^{-80}\ C\ m^6$. *ab initio* (Ref. 3): $Q_{2,0} = -4.487\ 10^{-40}\ C\ m^2$, $Q_{4,0} = -9.233\ 10^{-60}\ C\ m^4$, $Q_{6,0} = -6.129\ 10^{-80}\ C\ m^6$.
[b]$e = 1.602\ 10^{-19}\ C$.
[c]Optimized force centers $z_{SR} = \pm 0.0554$ nm practically coincide with the nuclear positions $z_N = \pm 0.0547$ nm.
[d]In parentheses: optimized parameter C if the force centers are fixed on the nuclei, $z_D = \pm 0.0547$ nm.

of the exponential and the r^{-6} site–site potentials have been allowed to shift (independently) along the N–N axes. The (three parameter) point charge model could in principle represent the first three nonzero multipole moments of N_2; in fact, it can do this only if they satisfy the relation: $Q_{2,0}Q_{6,0} \leq (Q_{4,0})^2 \leq \frac{4}{3}Q_{2,0}Q_{6,0}$, which does not hold for the calculated multipole moments of N_2.[3] We have fitted the site–site potential parameters to the *ab initio* results, calculated for six orientations and six distances $0.30 \leq R \leq 0.44$ nm. The fits have been performed in three separate steps, just as for ethylene,[18] in order to avoid correlation between the fit parameters.

(i) The charges $q = q_+ = -q_-$ and the position parameters z_+ and z_- have been found by fitting $\sum_i \sum_j q_i q_j r_{ij}^{-1}$ to $\Delta E^{(1)}_{\text{mult}}$, calculated up to R^{-9} terms inclusive, using the multipole moments of Ref. 3 (mean deviation 6.5% for 36 points).

(ii) The parameter $C = C_{N-N}$ and the positional parameter of the r^{-6} force centers have been found by fitting $\sum_i \sum_j C r_{ij}^{-6}$ to $\Delta E^{(2)}_{\text{mult}}$, calculated up to R^{-10} terms inclusive from the multipole coefficients of Ref. 3, Table VI, (mean deviation 6.3%, or 9.7% if the force centers were fixed on the nuclei).

(iii) The sum of the short range contributions $\Delta E^{(1)}_{\text{pen}}$ and $\Delta E^{(1)}_{\text{exch}}$, emerging from the present *ab initio* calculations, has been fitted by the exponential site–site potential $\sum_i \sum_j A \exp(-B r_{ij})$. Both short range components indeed appear to behave as an exponential. This has yielded the parameters $A = A_{N-N}$ and $B = B_{N-N}$ (mean deviation 9.2%); the optimum positions of the force centers practically coincide with the nuclear positions, in this case.

The results have been listed in Table III. We conclude that for N_2–N_2 the generalized atom–atom (site–site) potential forms a rather good representation of the *ab initio* results (see also Figs. 3 and 4). Especially for the short range interactions, the fit is much better than for the ethylene case.[18] Possibly this is due to the effect of the nitrogen lone pair electrons balancing the effects of chemical bonding on the charge distribution. [The fact that the intermolecular interaction is not an additive (isotropic) atom–atom interaction is caused, of course, by the chemical bonding.] Also for a much

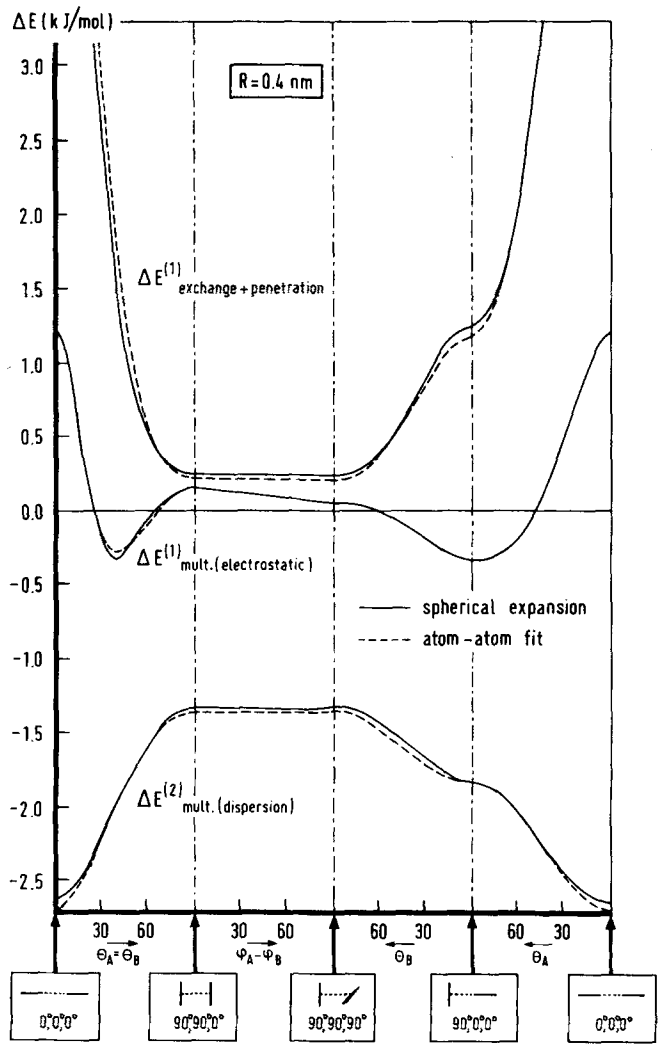

FIG. 3. Orientational dependence of different long range (multipole) and short range (penetration plus exchange) contributions to the interaction energy, at $R = 0.4$ nm. Spherical expansion, see Table V. Atom–atom potential I of Table III.

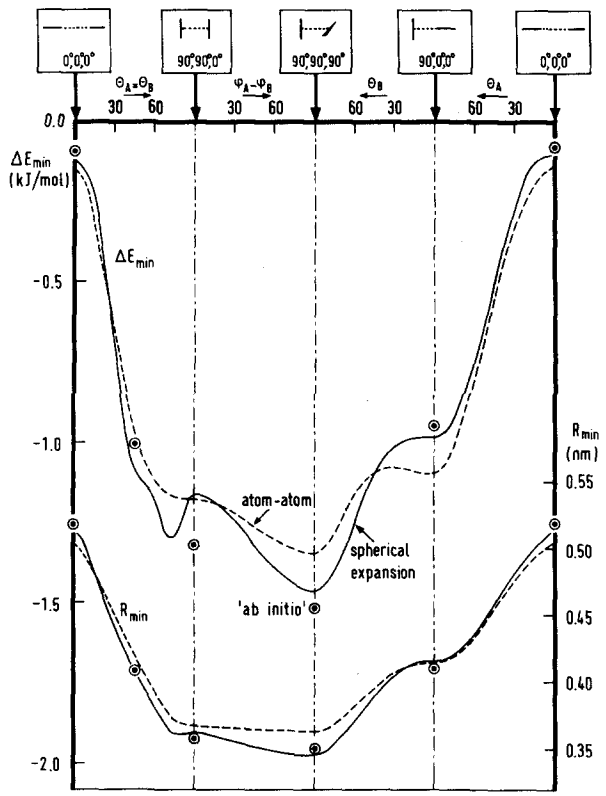

FIG. 4. Orientational dependence of the van der Waals minimum. The well depth ΔE_{min} and equilibrium distance R_{min} have been obtained by varying R for each orientation θ_A, θ_B, ϕ_A. *"Ab initio,"* spherical expansion, and atom–atom potentials defined as in Figs. 2 and 3.

larger set of orientations where the N_2–N_2 interaction potential has been calculated *ab initio* (see below), the site–site potential yields a rather good description of the anisotropy (see Sec. IV, Table IV).

C. Spherical expansion of the *ab initio* potential by numerical integration

Since the site–site potential yields a rather good description of the *ab initio* calculated N_2–N_2 potential, we can now use the first in order to obtain a reliable spherical expansion of the latter. First, we have made a spherical expansion of the site–site potential. For this known potential the expansion coefficients can be obtained from formula (4), by performing the angular integration. This integration can be considerably simplified. (1) Using the invariance of ΔE and $A_{L_A,L_B,L}$ under rotations of the total system reduces the integration to the three "internal" angles θ_A, θ_B, ϕ_A ($\Theta=\Phi=\phi_B=0$). The angular functions can be written as:

$$A_{L_A,L_B,L}=\left(\frac{(2L_A+1)(2L_B+1)(2L+1)}{64\pi^3}\right)^{1/2}\sum_{M_A=0}^{L_B}(2-\delta_{M_A,0})\times\left(\frac{(L_A-M_A)!(L_B-M_A)!}{(L_A+M_A)!(L_B+M_A)!}\right)^{1/2}\begin{pmatrix}L_A & L_B & L\\ M_A & -M_A & 0\end{pmatrix}\times P_{L_A}^{M_A}(\cos\theta_A)P_{L_B}^{M_A}(\cos\theta_B)\cos M_A\phi_A\,,$$

where the P_L^M are associated Legendre functions.[14] (2) Using the symmetry properties of the system reduces the integration intervals. Since the angular functions depend only on $\cos\theta_A$, $\cos\theta_B$, and $\cos\phi_A$ (the function $\cos M_A\phi_A$ can easily be expanded as a function of $\cos\phi_A$) and the volume element is $d(\cos\theta_A)d(\cos\theta_B)d\phi_A$ one can substitute $\eta_A=\cos\theta_A$, $\eta_B=\cos\theta_B$, and $\zeta_A=\cos\phi_A$ and obtain the integral

$$V_{L_A,L_B,L}(R)=8\pi^{1/2}\int_0^1 d\eta_A\int_0^1 d\eta_B\int_{-1}^1 d\zeta_A(1-\zeta_A^2)^{-1/2}\times A_{L_A,L_B,L}(\eta_A,\eta_B,\zeta_A)\Delta E(\arccos\eta_A,\arccos\eta_B,\arccos\zeta_A;R)\,.$$

This integral is very suitable for numerical integration. The best method for our purpose (which is to apply it to *ab initio* results) is one of the Gaussian integration techniques, since these give the highest accuracy with the smallest number of integration points.[19] For Legendre functions it is best to choose the Gauss–Legendre modification. (Parker *et al.*[20] have used this technique in a one-dimensional integration required to obtain the Ar–CO potential.) We have used formulas (25.4.30) and (25.4.38) of Ref. 21. Since we only have to find the spherical expansion of the short range contributions $\Delta E_{pen}^{(1)}$ and $\Delta E_{exch}^{(1)}$ (see Sec. III A), we have applied this integration method to the exponential part of the site–site potential, Sec. III B, term (iii). Some experimentation with the grid and with the expansion length has led to the following conclusions. (1) The first 18 terms in the spherical expansion are necessary to represent the short range potential to an accuracy better than one percent in each point. (2) The required number of integration points for (η_A, η_B, ζ_A) is (6, 6, 5).

TABLE IV. Spherical expansion coefficients Eq. (4) of the short range (penetration and exchange) interaction energy.

	$V^{SR}_{L_A,L_B,L}$ (kJ mol^{-1}) at $R=0.3$ nm	
L_A, L_B, L	*ab initio*[a]	atom–atom[b]
0, 0, 0	44.258	49.769
2, 0, 2	23.871	26.936
2, 2, 0	2.947	3.674
2, 2, 2	−4.734	−5.794
2, 2, 4	13.154	14.667
4, 0, 4	4.309	3.551
4, 2, 2	0.314	0.380
4, 2, 4	−0.732	−0.701
4, 2, 6	3.151	2.520
4, 4, 0	0.005	0.010
4, 4, 2	−0.006	−0.015
4, 4, 4	0.026	0.033
4, 4, 6	−0.131	−0.107
4, 4, 8	1.035	0.573
6, 0, 6	0.389	0.264
6, 2, 4	0.011	0.018
6, 2, 6	−0.057	−0.049
6, 2, 8	0.399	0.250

[a]Calculated by numerical integration from the *ab initio* data for a grid of 180 (105 independent) orientations (AO basis, see Table I).
[b]Same as Ref. a, for the repulsive part of the atom-atom potential II (Table III, exponential term).

TABLE V. Spherical expansion of the complete interaction potential [Eq. (3)].

$$V_{L_A,L_B,L}(R) = V^{SR}_{L_A,L_B,L}(0.3)\exp[-0.00153-35.6(R-0.3)-20.5(R-0.3)^2] + C^{L_A,L_B,L}_{L_A+L_B+1}R^{-(L_A+L_B+1)} + C^{L_A,L_B,L}_{6}R^{-6} + C^{L_A,L_B,L}_{8}R^{-8} + C^{L_A,L_B,L}_{10}R^{-10}.$$

R in nm; $V^{SR}_{L_A,L_B,L}(0.3)$ from Table IV, *ab initio*.

	Long range (multipole) coefficients[a]			
	Electrostatic	Dispersion		
	$C^{L_A,L_B,L}_{L_A+L_B+1}$	$C^{L_A,L_B,L}_{6}$	$C^{L_A,L_B,L}_{8}$	$C^{L_A,L_B,L}_{10}$
L_A, L_B, L	(kJ mol^{-1} nm$^{L_A+L_B+1}$)	(kJ mol^{-1} nm^6)	(kJ mol^{-1} nm^8)	(kJ mol^{-1} nm^{10})
0, 0, 0	•••	$-4.231\ 10^{-3}$	$-2.946\ 10^{-4}$	$-2.239\ 10^{-5}$
2, 0, 2	•••	$-1.815\ 10^{-4}$	$-5.277\ 10^{-5}$	$-5.974\ 10^{-6}$
2, 2, 4	$1.849\ 10^{-3}$	$-3.638\ 10^{-5}$	$-4.932\ 10^{-6}$	$-1.219\ 10^{-6}$
2, 2, 2	•••	$-4.505\ 10^{-6}$	$1.026\ 10^{-6}$	$3.692\ 10^{-7}$
2, 2, 0	•••	$-3.764\ 10^{-6}$	$-6.098\ 10^{-7}$	$-2.256\ 10^{-7}$
4, 2, 6	$7.655\ 10^{-5}$	•••	•••	•••
4, 4, 8	$6.078\ 10^{-6}$	•••	•••	•••
6, 2, 8	$8.465\ 10^{-7}$	•••	•••	•••

[a]Note that the long range multipole coefficients $C^{L_A,L_B,L}_n$ defined in this paper are different from the $C^{L_A,L_B,M}_n$ of Ref. 3; the two definitions are, of course, related by a simple linear transformation.

Next we have performed *ab initio* calculations of $\Delta E^{(1)}$ [Eq. (1)] at these grid points.[21] (Using the full symmetry their number can be further reduced from 180 to 105). The intermolecular distance for which we have chosen to do this is $R=0.3$ nm, since this distance is relevant both for beam scattering experiments and for solid state properties.[2] The expansion coefficients which result from the numerical integration of the *ab initio* points are given in Table IV.

We observe that the short range coefficients $V^{SR}_{L_A,L_B,L}$ indeed decrease with increasing L_A and L_B; the expansion is convergent. Most of the terms with L_A, $L_B=4$, 4 and 6, 2 are less than 1% of the isotropic coefficient $V^{SR}_{0,0,0}$. For fixed L_A, L_B the coefficients increase with increasing L. The 18 term expansion deviates less than 0.5% from the *ab initio* results; truncation of the series after L_A, $L_B=4$, 4 leads to an error of 2%; truncation after L_A, $L_B=2$, 2 to 16% error.

If one wants to determine the distance dependence of the expansion coefficients $V^{SR}_{L_A,L_B,L}(R)$ this procedure should be repeated for a set of distances R. The *ab initio* calculations are rather expensive, however, (about 3 h of IBM 370/158 CPU time per point) and so we have instead used a different, more approximate method. We have assumed that all expansion coefficients $V^{SR}_{L_A,L_B,L}$ of the short range energy have the same exponential distance dependence:

$$V^{SR}_{L_A,L_B,L}(R) \simeq \tilde{V}^{SR}_{L_A,L_B,L}(R) \equiv V^{SR}_{L_A,L_B,L}(R_0)\exp[A-B_1(R-R_0)-B_2(R-R_0)^2],$$

with $R_0=0.3$ nm. The parameters A, B_1, and B_2 have been optimized by fitting the spherically expanded $\Delta\tilde{E}^{(1)}$ with the coefficients given by $\tilde{V}^{SR}_{L_A,L_B,L}(R)$ to the *ab initio* values of $\Delta E^{(1)}_{pen}+\Delta E^{(1)}_{exch}$ calculated for six orientations and six distances $0.3\le R\le 0.44$ nm. The accuracy of the fit is 7%; the results (see Table V), in combination with the long range results,[3] yield a fairly good representation of the *ab initio* calculations for the N_2–N_2 interaction potential (see Figs. 2 and 4).

IV. APPLICATIONS OF THE N_2–N_2 INTERACTION POTENTIAL; COMPARISON WITH EXPERIMENTAL DATA

A. Isotropic potential

Our calculated isotropic N_2–N_2 potential, $V_{0,0,0}(R)$, can be compared with some empirical isotropic potentials from gas phase virial coefficients, viscosity data, and from solid state properties.[22] Since the latter have only been determined in the simplified forms of Lennard–Jones (12-6) or Buckingham (exp – 6) potentials, we shall not compare the shape of the potentials but only their main characteristics: the scattering diameter (σ), the equilibrium distance (R_m), and the well depth (ΔE_m). The results listed in Table VI show that the agreement is good, so that we expect our calculated potential to explain quantitatively the experimental bulk data (at least those which have been used to determine the empirical potential parameters).

B. N_2 crystal properties

Our site–site potential fitted to the *ab initio* data (Sec. III B) has been used to calculate the equilibrium structure and the cohesion energy of the ordered (α and γ) phases of solid N_2. The results, unit cell dimension $a=0.561$ nm for the cubic α phase, cohesion energy 6.43 kJ/mol (corrected for the zero-point lattice vibrations), and $a=0.403$ nm, $c=0.500$ nm for the tetragonal γ phase, are in good agreement with the experimental data,[1,2] $a=0.564$ nm, heat of sublimation (at 0 °K) 6.92 kJ/mol for α-N_2, $a=0.396$ nm, $c=0.510$ nm for γ-N_2. Also the phonon frequencies at various wave vectors, obtained from harmonic or self-consistent phonon lattice

TABLE VI. Characteristics of the isotropic potential.

	σ (nm)	R_m (nm)	ΔE_m (kJ mol^{-1})
Calculated $V_{0,0,0}(R)$ (Table V)	0.376	0.417	0.748
Lennard–Jones (12-6) from virial coefficients (Ref. 22, p. 209)	0.370	0.415	0.793
Lennard–Jones (12-6) from viscosity data (Ref. 22, p. 209)	0.368	0.413	0.763
Buckingham (exp – 6) from virial coefficients and crystal data (Ref. 22, p. 181)	0.363	0.404	0.947
Buckingham (exp – 6) from viscosity data (Ref. 22, p. 181)	0.362	0.401	0.844

dynamics calculations using our nonempirical site–site potential, agree nicely with the experimental data. Further details will appear in a forthcoming paper,[23] which is concerned with the properties of solid N_2 in the α and γ phases and their temperature and pressure dependence.

C. Stability and structure of $(N_2)_2$

In the gas phase at 77 °K stable N_2 dimers, so-called van der Waals molecules, have been observed and their infrared spectrum has been measured.[24] In spite of this knowledge of the spectrum, the structure of this N_2 dimer has not been established. Mainly on the basis of favorable quadrupole–quadrupole interactions a T-shaped equilibrium structure ($\theta_A = 90°$, $\theta_B = \phi_A = 0°$) has been proposed.[24] Addition of the higher multipole interactions plus the anisotropic dispersion interactions from *ab initio* calculations gives further support for the stability of this T-shaped complex, but also suggests another possible structure of equal stability, the staggered parallel one ($\theta_A = \theta_B \simeq 45°$, $\phi_A = 0°$).[3] A more approximate model including the short range repulsion[25] predicts a T-shaped or a crossed ($\theta_A = \theta_B = \phi_A = 90°$) $(N_2)_2$ structure, but if the molecular shape parameters are somewhat modified the outcome is a T-shaped or a staggered parallel structure.[26] Beam deflection measurements,[27] which are sensitive to the dipole moment of the molecular complex, have not demonstrated the existence of such a dipole on $(N_2)_2$. Several possible $(N_2)_2$ structures must have a zero dipole, however, because of symmetry (for instance, the staggered parallel one and the crossed one), and for the remaining structures (such as the T-shaped) the interaction induced dipole may be too small to be detectable.

With our quantitative knowledge of the anisotropic N_2–N_2 interaction potential, including both the long range and the short range contributions, we can make somewhat more definite remarks on the N_2 dimer structure and confront these with the available experimental information. To this end we have studied the potential surface of $(N_2)_2$ as a function of the internal angles θ_A, θ_B, and ϕ_A and the distance R. It is of course not possible to present the complete hypersurface pictorially. In Figs. 2 and 4 we have shown some typical cuts through the surface; Fig. 3 displays the angular dependence of the different long range and short range contributions to the potential. Especially Fig. 4 contains much information since the distance R has been varied to find the energy minimum $\Delta E_{\min}$ of $(N_2)_2$ and the equilibrium distance $R_{\min}$ for each orientation (θ_A, θ_B, ϕ_A). In Fig. 3 we observe that, indeed, the T-shaped and the staggered parallel structure have maximum electrostatic attraction. The dispersion energy is most favorable, of course, for the linear structure ($\theta_A = \theta_B = \phi_A = 0°$). For distances in the neighborhood of the van der Waals minimum the short range exchange repulsion is the dominant anisotropic term, however. Since it increases very steeply when the molecular charge clouds start to overlap (especially in the linear structure), it determines to a large extent the distance of closest approach of the molecules. If, for a given orientation, the long range interactions are not maximally attractive (when compared with other orientations, for equal distance R), but the molecules can approach each other closely, the van der Waals well may still be relatively deep. This is, for instance, what happens for the crossed $(N_2)_2$ structure. In general, one can observe this role of the short range repulsion from Fig. 4, where the well depth $\Delta E_{\min}$ shows a strong correlation with the equilibrium distance $R_{\min}$. Only when the short range repulsion is not very sensitive to a change of orientation (for instance, the rotation over ϕ_A in the N_2 dimer with $\theta_A = \theta_B = 90°$, see Fig. 3) the long range interactions (in this case, the electrostatic ones, even though they are repulsive) can still be important in determining the equilibrium structure.

This crucial role of the short range interactions for the dimer structure (leading to closest packing) may suggest that the structure of nearest neighbor pairs in the molecular crystal forms a good indication for the equilibrium structure of the van der Waals dimer. This has indeed been suggested.[28] Our results (see Table VII) demonstrate, however, that maximum binding energy for the N_2 dimer does not occur for the nearest neighbor orientations from the crystal. In fact, it is not obvious, even if only packing considerations determine the structure, that the optimum packing in a crystal where each molecule is surrounded by several neighbors must correspond with optimally packed dimers. The crystal neighbors should not have too unfavorable pair energies, though, but the results in Table VII show that this is not the case.

The absolute minimum in our N_2–N_2 potential surface (a complete search is made using the site–site potential, a cruder one on the spherically expanded potential), occurs for the crossed structure at $R = 0.35$ nm and $\Delta E \simeq 1.5$ kJ/mol (see Table VII). This minimum lies considerably closer and deeper than the minimum of the isotropic potential ($R_m = 0.417$ nm, $\Delta E = 0.75$ kJ/mol). The equilibrium distance is close to the value ($R = 0.37$ nm) inferred from the infrared spectrum,[24] but the T-shaped structure proposed in this paper[24] has not been confirmed, due to the anisotropy of the short range repulsions. (Actually, our minimum for the

TABLE VII. $(N_2)_2$ structure and binding energy.

	R (nm)	θ_A	θ_B	ϕ_A	ΔE (kJ mol^{-1})
Most stable dimer structure[a]	0.364[a] (0.346,[b] 0.350[c])	90°	90°	90°	1.35[a] (1.46,[b] 1.52[c])
α-N_2 crystal[d] neighbor pair	0.399 (0.404[e])	90°	35°	55°	1.05 (1.05[e])
γ-N_2 crystal[d] neighbor pair	0.379 (0.398[e])	90°	42°	90°	0.94 (1.09[e])

[a]Neglecting the energy of the nuclear motions; complete search of the potential energy surface has been performed with the atom–atom potential I of Table III.
[b]From the spherical expansion, Table V.
[c]From the *ab initio* first order energy (Table I) and the second order energy from the dispersion multipole coefficients of Ref. 3 (Table VI), see Table V and Fig. 2.
[d]Experimental crystal structure, see Ref. 1, nearest neighbor pair energy ΔE calculated with atom–atom potential I.
[e]R_{min} and ΔE_{min} obtained with the atom–atom potential I (Table III) for fixed N_2 orientations from Ref. d.

T-shaped structure lies much further outwards, at $R = 0.42$ nm). The potential surface is rather flat around the minimum, however; the balance between the attractive and repulsive contributions is subtle and different possible structures are near in binding energy. In some directions the barriers for internal N_2 rotations are rather low; for instance, for a complete rotation over ϕ_A in the dimer with $\theta_A = \theta_B = 90°$ it is about 0.2 kJ/mol (17 cm^{-1}) with practically no variation of the equilibrium distance (see Fig. 4). This agrees nicely with the estimate of 15 to 30 cm^{-1} from the IR spectrum.[24] So we expect the N_2 molecules in the dimer to make rather wide angular oscillations (librations) or, maybe, hindered rotations (the rotational constant of free N_2 is 2.0 cm^{-1}). This is comparable to the situation in the plastic crystal phase, β-N_2. In other directions, rotations of the molecules are strongly quenched; the complex must almost dissociate before such a rotation becomes possible (for instance, rotations through the linear structure, see Fig. 4). Before we can make a conclusive comparison with the experimental spectrum, we have to solve the dynamical problem for the nuclear motions, which may be not an easy job in this case.

Note added in proof. After completion of this manuscript we have received a preprint by Ree and Winter,[29] also containing *ab initio* results for the N_2–N_2 potential. These authors have concentrated on the short range, strongly repulsive, region of the potential. The smaller basis set which they have used (overestimating, for instance, the N_2 quadrupole moment), in combination with the supermolecule self-consistent field (SCF) method (leading to some basis set superposition error), is less adequate for the long range and for the region of the van der Waals minimum, on which we have concentrated. Moreover, they have not included the dispersion energy contribution.

ACKNOWLEDGMENTS

We are most grateful to Dr. Paul E. S. Wormer for his critical reading of the manuscript and for many very stimulating discussions. Also we acknowledge valuable discussions with Dr. Fred Mulder and Dr. Tadeusz Luty. The University Computing Center is thanked for a generous supply of facilities. We thank Dr. F. H. Ree and Dr. N. W. Winter for communicating their results prior to publication.

[1]T. A. Scott, Phys. Rep. **27C**, 89 (1976), and references therein.
[2]J. C. Raich and N. S. Gillis, J. Chem. Phys. **66**, 846 (1977), and references therein.
[3]F. Mulder, G. van Dijk, and A. van der Avoird, Mol. Phys. **39**, 407 (1980).
[4]P. E. S. Wormer, thesis, University of Nijmegen, 1975.
[5]P. E. S. Wormer, F. Mulder, and A. van der Avoird, Int. J. Quantum Chem. **11**, 959 (1977).
[6]G. Herzberg, *Spectra of diatomic molecules* (Van Nostrand, New York, 1950).
[7]B. Jeziorski and W. Kolos, Int. J. Quantum Chem. **12S1**, 91 (1977).
[8]P. W. Langhoff, M. Karplus, and R. P. Hurst, J. Chem. Phys. **44**, 505 (1966).
[9]F. Mulder, A. van der Avoird, and P. E. S. Wormer, Mol. Phys. **37**, 159 (1979).
[10]K. C. Ng, W. J. Meath, and A. R. Allnatt, Mol. Phys. **33**, 699 (1977).
[11]W. A. Steele, J. Chem. Phys. **39**, 3197 (1963).
[12]A. J. Stone, Mol. Phys. **36**, 241 (1978).
[13]A. van der Avoird, P. E. S. Wormer, F. Mulder, and R. M. Berns, in *Van der Waals systems*, edited by R. Zahradnik, *Topics in Current Chemistry* (Springer, Berlin, 1980).
[14]D. M. Brink and G. R. Satchler, *Angular momentum*, 2nd ed. (Clarendon, Oxford, 1975).
[15]P. J. M. Geurts, P. E. S. Wormer, and A. van der Avoird, Chem. Phys. Lett. **35**, 444 (1975).
[16]P. C. Hariharan and W. Kutzelnigg, Progress Rept. Lehrstuhl für Theoretische Chemie, Ruhr-Universität, Bochum (1977).
[17]J. Schaefer and W. Meyer, J. Chem. Phys. **70**, 344 (1979).
[18]T. Wasiutynski, A. van der Avoird, and R. M. Berns, J. Chem. Phys. **69**, 5288 (1978).
[19]T. Stoer, *Einführung in die numerische Mathematik*, (Springer, Berlin, 1972), Vol. I.
[20]G. A. Parker and R. T Pack, J. Chem. Phys. **69**, 3268 (1978).
[21]M. Abramowitz and I. A. Stegun, *Handbook of Mathematical Functions* (Dover, New York, 1968).
[22]J. O. Hirschfelder, C. F. Curtiss, and R. B. Bird, *Molecular Theory of Gases and Liquids*, 2nd ed. (Wiley, New York,

1964).
[23]T. Luty, A. van der Avoird, and R. M. Berns (to be published).
[24]C. A. Long, G. Henderson, and G. E. Ewing, Chem. Phys. 2, 485 (1973).
[25]A. Koide and T. Kihara, Chem. Phys. 5, 34 (1974).
[26]K. Sakai, A. Koide, and T. Kihara, Chem. Phys. Lett. 47, 416 (1977).
[27]S. E. Novick, P. B. Davies, T. R. Dyke, and W. Klemperer, J. Am. Chem. Soc. 95, 8547 (1973).
[28]J. M. Steed, T. A. Dixon, and W. Klemperer, J. Chem. Phys. 70, 4940 (1979).
[29]F. H. Ree and N. W. Winter, J. Chem. Phys. (submitted for publication).